

https://doi.org/10.1070/QEL17089

Continuous-wave laser diodes based on epitaxially integrated InGaAs/AlGaAs/GaAs heterostructures

M.A. Ladugin, N.V. Gul'tikov, A.A. Marmalyuk, V.P. Konyaev, A.V. Solov'eva

Abstract. **We report the results of the development and investigation of the main characteristics of integrated laser emitters for the spectral range from 1040 to 1080 nm. These devices are fabricated using epitaxially integrated InGaAs/AlGaAs/GaAs heterostructures with one or two emitting regions, and measurements are performed in pulsed, quasi-continuous, and continuous-wave pump regimes. It is found that along with the obvious advantage of integrated emitters – an increase in the output optical power, they also have a significant limitation, which consists in increasing the amount of released heat. Despite this, it is shown that such integrated double laser diodes operate efficiently in the continuous-wave generation regime ($P_{max} \sim 6$ W), demonstrating a 1.7-fold increase in the differential quantum efficiency as compared to single laser diodes.**

Keywords: *laser diode, epitaxially integrated heterostructure, continuous-wave regime, heat release.*

1. Introduction

Over the past few decades, increasing the output optical power of semiconductor laser emitters has continued to be one of the key directions in the development of modern optoelectronics. Several different ways have been demonstrated to improve the emission parameters of laser diodes (LDs), which are characterised by their own characteristics. An increase in the output power obtained from a single crystal can be achieved by optimising the geometry of laser heterostructures, as well as improving the design and manufacturing technology of the active element and the methods of its installation. In the general case, each of the methods involves reducing spurious radiation losses inside and outside the laser structure in order to decrease the amount of released heat and increase the differential quantum efficiency and the efficiency of the device.

One of the promising methods for increasing the output optical power, presented and discussed in this work, is the fabrication of epitaxially integrated LDs with several emitting regions. In addition to high optical power, which is determined by the number of emitting regions, these LDs are capable of emitting at several wavelengths.

M.A. Ladugin, N.V. Gul'tikov, A.A. Marmalyuk, V.P. Konyaev, A.V. Solov'eva Open Joint-Stock Company 'M.F. Stel'makh Polyus Research Institute', ul. Vvedenskogo 3, korpus 1, 117342 Moscow, Russia; e-mail: maximladugin@mail.ru, m.ladugin@siplus.ru

Received 27 June 2019
Kvantovaya Elektronika **49** (10) 905–908 (2019)
Translated by I.A. Ulitkin

Previously, the high efficiency of such lasers made of epitaxially integrated heterostructures emitting in the spectral range from 800 to 1600 nm was successfully demonstrated during their operation in the pulsed pump regime [1–4]. Moreover, despite an increase in the pulse repetition rate to tens of kilohertz or their use in multi-element emitters [5], a noticeable decrease in the output parameters of integrated LDs was not observed during operation. This is due to the fact that during one pulse, the duration of which is usually 100 ns, the temperature of the active regions does not have time to increase to a level where its negative effect on the threshold current density and external differential quantum efficiency becomes noticeable.

Nevertheless, it is still difficult to produce high-power integrated lasers operating in quasi-continuous and continuous-wave pump regimes, which are characterised by increased heat release. This is due to a significant overheating of the active regions, which leads to an increase in the threshold current density, an increase in optical losses, and a decrease in the external differential quantum efficiency of the entire emitter. Thus, Patterson et al. [6] demonstrated the possibility of obtaining continuous-wave generation of double laser diodes at room temperature, but the maximum power of such emitters reached only about 10 mW from one face (in terms of the strip contact width of 10 μm).

The present work is devoted to the study of the functioning of integrated LDs with several emitting regions operating in different pump regimes, as well as to the search for the possibility of increasing their output optical power.

2. Experimental samples

Epitaxially integrated heterostructures were grown by MOCVD in a single growth cycle. Carefully selected growth regimes allowed us to produce active, waveguide and emitter layers, as well as tunnel junctions of good quality. The geometry of the InGaAs/AlGaAs/GaAs heterostructure was chosen to ensure subsequent laser generation at a wavelength of 1060 nm with a narrow radiation pattern. A single structure (single laser) was grown to control and compare laser parameters. The band diagram of the integrated (double) laser is schematically shown in Fig. 1.

The active element had an electric contact width W = 100–200 μm, a cavity length L = 1.0–1.4 mm, and mirror reflection coefficients $R_1 = 0.04$ and $R_2 = 0.96$. Laser elements were fabricated according to standard technology, the crystal being mounted p-down onto the heat sink according to the technique described in [2, 4]. The measurements were performed in various current pump regimes with a pulse duration from 100 ns to continuous.

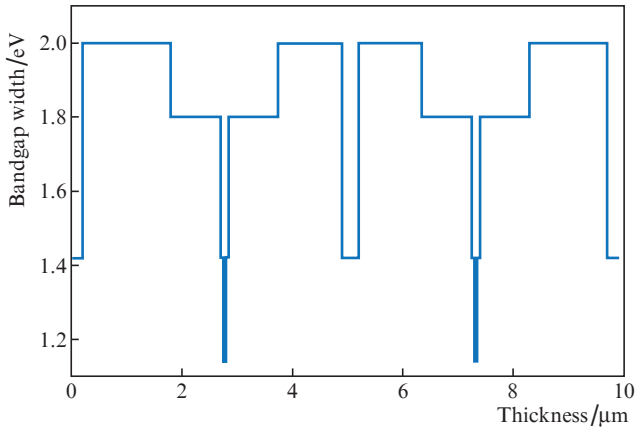

Figure 1. Schematic representation of the band diagram of an epitaxially integrated double LD.

3. Results and discussion

Laser emitters with one and two active regions were preliminary tested in a pulsed pump regime (τ = 100 ns, ν = 1 kHz), and their emission spectra contained only one maximum, which indicated the absence of noticeable overheating (Fig. 2a) In this case, to determine the overheating, we used the experimentally obtained values of $\delta\lambda/\delta T$, amounting to $\sim$0.32 nm K^{-1} (Fig. 2b). It is worth noting that the assessment of temperature in this way differed from direct measurement of the active region temperature by no more than 10% [7].

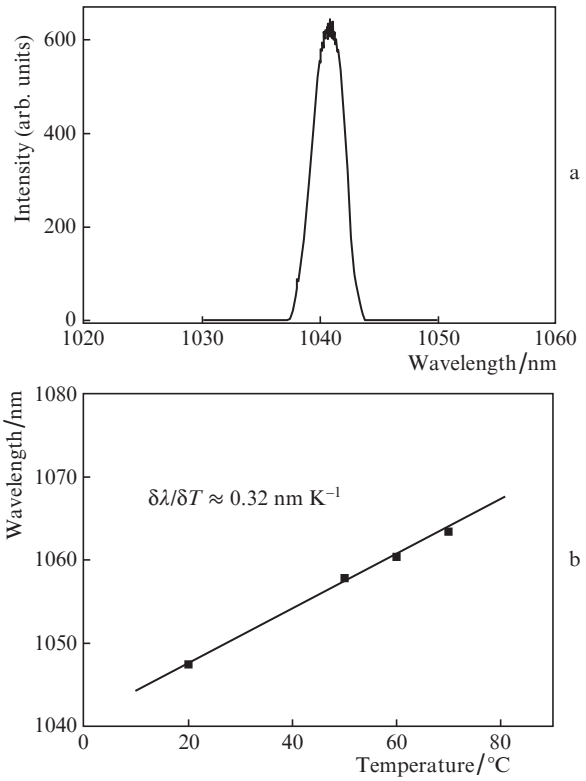

Figure 2. (a) Emission spectrum of an LD with two active regions, measured in the pulsed pump regime (100 ns, 1 kHz) and (b) temperature dependence of the laser diode generation wavelength, measured in the continuous-wave regime at a current I = 3 A.

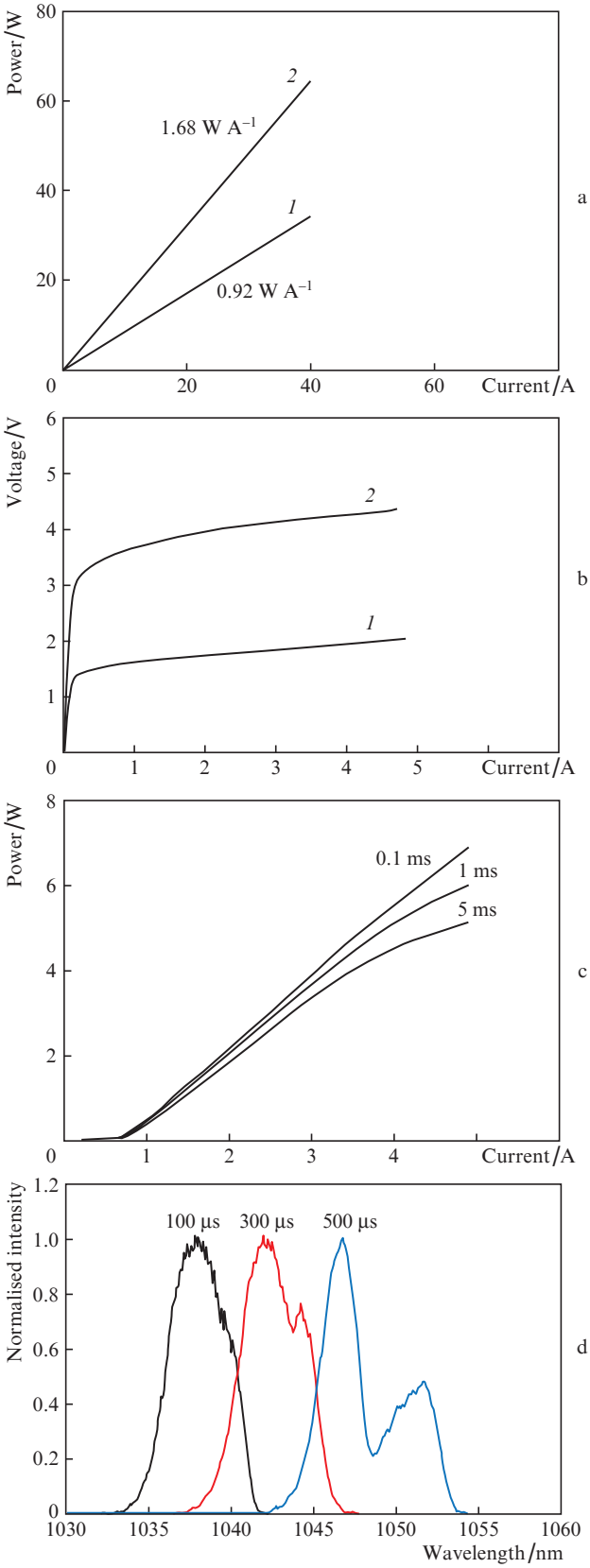

Figure 3. (a) Light–current characteristic of (*1*) single and (*2*) double LDs in the pulsed pump regime (τ = 100 ns, ν = 1 kHz); (b) current–voltage characteristic of (*1*) single and (*2*) double LDa; (c) light–current characteristic of a double LD in the quasi-continuous pump regime (ν = 100 Hz) at pulse durations of 0.1, 1 and 5 ms; (d) emission spectra of a double LD in the quasi-continuous pump regime (ν = 1.5 kHz) at pulse durations of 100, 300, and 500 μs.

The light–current (L–I) and current–voltage (I–V) characteristics measured in the pulsed regime demonstrate an increase in both the output optical power and the cutoff voltage of a double laser (Figs 3a and 3b). Figures 3c and 3d show the light–current and spectral characteristics of a double laser, measured in the quasi-continuous regime at a fixed repetition rate, but different durations, of pump pulses. It follows from the figure that with an increase in the pulse duration, the power decreases more strongly, which indicates the heating of the active region during a single pulse. This is clearly seen on the emission spectra of the LD (Fig. 3d). If with a short duration only one maximum was observed in the spectrum, then with its increase, the spectrum shifted noticeably to the red and already had two maxima caused by a higher temperature of the active region located farther from the heat sink.

Continuous-wave generation of a double laser was obtained, and the linearity of its L–I characteristic remained at about 4 W; in this case, the L–I characteristic slope was 1.64 W A^{-1}, which is 1.7 times higher than that of a single LD (Fig. 4a). However, at a pump current of more than 3–4 A, a significant overheating of the active regions of the integrated LD was observed, which we assessed to reach 100–120 °C. This caused a nonlinearity of the L–I characteristic and limited the level of the maximum attainable radiation power.

Figure 4b shows the spectral characteristics of epitaxially integrated LDs at various injection currents in the continuous-wave regime. One can see that with increasing current from the threshold value (I_{th} = 0.6 A), the emission spectrum not only shifts to the red, but also splits into two separate maxima. Moreover, with a further increase in current, these maxima more and more differ from each other in wavelength.

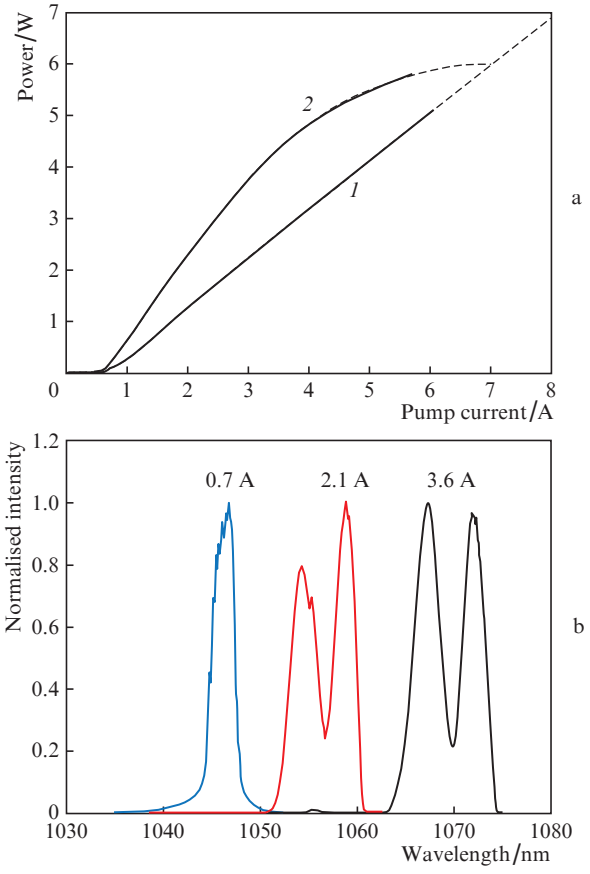

Figure 4. (a) Light–current characteristics in the continuous-wave generation regime for (*1*) single and (*2*) double LDs and (b) radiation intensity spectra for double LDs in the continuous-wave generation regime at pump currents of 0.7, 2.1, and 3.6 A.

A calculated estimate of the active region temperature for double LDs of various designs was performed by solving the unsteady heat equation with internal heat sources:

$$c_v \frac{\partial T(\boldsymbol{x},t)}{\partial t} = \nabla(\varkappa \nabla T(\boldsymbol{x},t)) + q_v(\boldsymbol{x},t),$$

$$\boldsymbol{x} \in \Omega \subset \mathbb{R}^3,\ t > 0,$$

where $\boldsymbol{x} = (x,y,z)^T$ is the radius vector of a point; t is the time; T is the temperature; c_v is the volumetric heat capacity of the material ($c_v = c\rho$, where c is the mass heat capacity and ρ is the density of the material); $\varkappa$ is the coefficient of thermal conductivity; q_v is the volume density of internal sources; ∇ is the Hamilton differential operator; and Ω is some closed region in three-dimensional space.

At one of the faces of the heat sink, a constant temperature (T_b) is maintained, for which a boundary condition of the first kind is valid: T_b = const. To simplify, this model does not take into account convective and conductive methods of heat exchange with the environment. All faces, both of the heat sink and the LD, are in contact with the environment and are thermally isolated (except for the face with a constant temperature). A boundary condition of the second kind is valid for them, which in this case is defined as

$$\left.\frac{\partial T}{\partial n}\right|_w = 0,$$

where n is the external normal to the boundary of the computational domain, and the index w means the boundary of the computational domain. The initial heat transfer condition has the form

$$T(t=0) = T_0.$$

Figure 5 schematically shows the three-dimensional structure of an LD with two active regions. To simplify, the heat

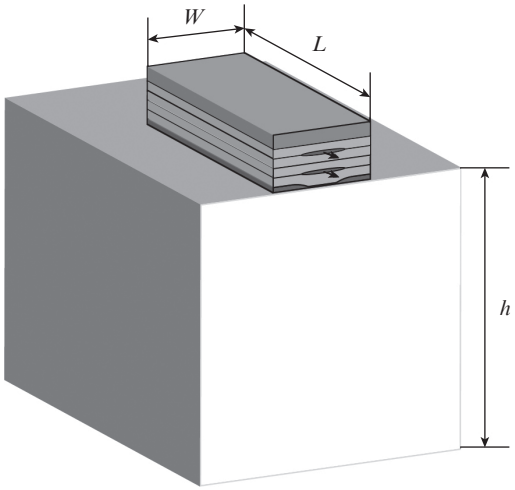

Figure 5. Geometry of a laser diode with two active regions on a copper heat sink.

source is the active region of the laser emitter. A copper cube with an edge size $h = 2$ mm was used as a heat sink for LDs of various designs. Despite a number of adopted simplifications, such calculations allow us with sufficient accuracy to estimate the temperature distribution in a single-laser crystal [7]. Here, a similar approach was developed to estimate the active region temperature of double epitaxially integrated LDs.

Figures 6a and 6b present the results of calculating the overheating of the active region for single and double LDs. The calculated temperature values are very close to the experimental ones. Therefore, this model makes it possible to fairly accurately predict temperature values for both single and double LDs, with the exception of the region of large overheating.

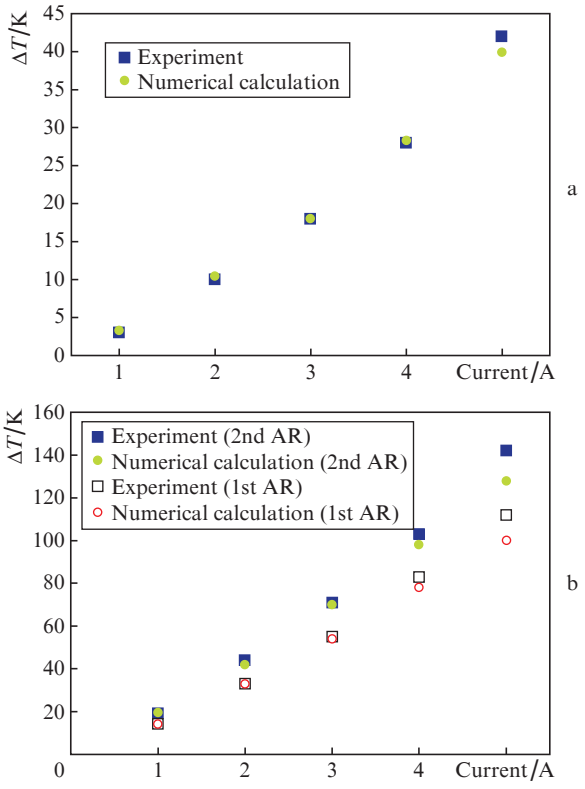

Figure 6. (a) Overheating ΔT of the active region (AR) of a single LD in the continuous-wave pump regime (experiment and numerical calculation) and (b) overheating of the active regions of a double LD in the continuous-wave pump regime (experiment and numerical calculation, the 1st active region is closer to the heat sink).

The results showed that the ultimate power of the devices is limited by the thermal saturation of the light–current characteristic rather than by the destruction of the active channel or the optical degradation of the output mirror. Under experimental conditions, it occurs at an output optical power of about 6 W, when the heating of both active regions exceeds 120 °C. To increase the power of integrated LDs in the continuous-wave regime, more detailed optimisation of the heterostructure, geometry of the active element, as well as improvement of the method of its installation on a heat sink are required. For example, the calculated estimates of various designs of the heterostructure and the active element showed that due to the application of the approaches described in [8–10], the emitter efficiency should increase by 10%–15%, and the ultimate power in the continuous-wave regime can increase up to 10–11 W.

In addition, an optimised heat sink design with reduced thermal resistance to 4–5 K W^{-1} will further improve the output characteristics of such LDs in the continuous-wave generation regime.

Thus, we have developed and studied integrated continuous-wave LDs with an output power of 5–6 W. The effect of the current pump regime on the efficiency of the LD based on epitaxially integrated InGaAs/AlGaAs heterostructures with two emitting regions in the spectral range 1040–1080 nm has been analysed. The calculated and experimental results for single and double LDs have been compared. It has been shown that in continuous-wave regime at pump currents above 5 A, the heating of the active regions can exceed 100–120 °C. One way to increase power of such continuous-wave LDs is to optimise the design of the epitaxial heterostructure, active element, and heat sink.

References

1. Guo W., Shen G., Li J., Wang T., Gao G., Zou D. *Proc. SPIE*, **5623**, 217 (2005).
2. Davydova E.I., Zverkov M.V., Konyaev V.P., Krichevskii V.V., Ladugin M.A., Marmalyuk A.A., Padalitsa A.A., Simakov V.A., Sukharev A.V., Uspenskii M.B. *Quantum Electron.*, **39** (8), 723 (2009) [*Kvantovaya Elektron.*, **39** (8), 723 (2009)].
3. Boucher J.-F., Vilokkinen V., Rainbow P., Uusimaa P., Lyytikainen J., Ranta S. *Proc. SPIE Int. Soc. Opt. Eng.*, **7480**, 74800K (2009).
4. Marmalyuk A.A., Davydova E.I., Zverkov M.V., Konyaev V.P., Krichevsky V.V., Ladugin M.A., Lebedeva E.I., Petrov S.V., Sapozhnikov S.M., Simakov V.A., Uspenskiy M.B., Yarotskaya I.V., Pikhtin N.A., Tarasov I.S. *Semiconductors*, **45** (4), 519 (2011) [*Fiz. Tekh. Poluprovodn.*, **45** (4), 528 (2011)].
5. Konyaev V.P., Marmalyuk A.A., Ladugin M.A., Bagaev T.A., Zverkov M.V., Krichevsky V.V., Padalitsa A.A., Sapozhnikov S.M., Simakov V.A. *Semiconductors*, **48** (1), 99 (2014) [*Fiz. Tekh. Poluprovodn.*, **48** (1), 104 (2014)].
6. Patterson S.G., Petrich G.S., Ram R.J., Kolodziejski L.A. *Electron. Lett.*, **35** (5), 395 (1999).
7. Diehl R. *High-power Diode Lasers. Fundamentals, Technology, Applications* (Berlin, Heidelberg: Springer-Verlag, 2000).
8. Coldren L.A., Corzine S., Mashanovitch M. *Diode Lasers and Photonic Integrated Circuits* (Hoboken, New Jersey: John Wiley & Sons Inc, 2012).
9. Ladugin M.A., Marmalyuk A.A., Padalitsa A.A., Bagaev T.A., Andreev A.Yu., Telegin K.Yu., Lobintsov A.V., Davydova E.I., Sapozhnikov S.M., Danilov A.I., Podkopaev A.V., Ivanova E.B., Simakov V.A. *Quantum Electron.*, **47**, 291 (2017) [*Kvantovaya Elektron.*, **47**, 291 (2017)].
10. Ladugin M.A., Marmalyuk A.A. *Quantum Electron.*, **49**, 529 (2019) [*Kvantovaya Elektron.*, **49**, 529 (2019)].